
EFFICIENT ATTENTION-FREE VIDEO SHIFT TRANSFORMERS

Adrian Bulat

Samsung AI Center Cambridge
adrian@adrianbulat.com

Brais Martinez

Samsung AI Center Cambridge
brais.a@samsung.com

Georgios Tzimiropoulos

Samsung AI Center Cambridge
Queen Mary University London
g.tzimiropoulos@qmul.ac.uk

ABSTRACT

This paper tackles the problem of efficient video recognition. In this area, video transformers have recently dominated the efficiency (top-1 accuracy vs FLOPs) spectrum. At the same time, there have been some attempts *in the image domain* which challenge the necessity of the self-attention operation within the transformer architecture, advocating the use of simpler approaches for token mixing. However, there are no results yet for the case of video recognition, where the self-attention operator has a significantly higher impact (compared to the case of images) on efficiency. To address this gap, in this paper, we make the following contributions: (a) we construct a highly efficient & accurate attention-free block based on the shift operator, coined *Affine-Shift* block, specifically designed to approximate as closely as possible the operations in the MHSA block of a Transformer layer. Based on our Affine-Shift block, we construct our Affine-Shift Transformer and show that it already outperforms all existing shift/MLP-based architectures for ImageNet classification. (b) We extend our formulation in the video domain to construct Video Affine-Shift Transformer (VAST), the very first purely attention-free shift-based video transformer. (c) We show that VAST significantly outperforms recent state-of-the-art transformers on the most popular action recognition benchmarks for the case of models with low computational and memory footprint. Code will be made available.

1 INTRODUCTION

Video recognition is the problem of recognizing specific events of interest (*e.g.* actions, highlights) in video sequences. Compared to the image recognition problem, video recognition must address at least one additional important technical challenge: the incorporation of the time dimension induces significant computational overheads as, typically, in the best case, a temporal model has $T \times$ more complexity than its corresponding image counterpart (T is the number of frames in the video sequence)¹. For example, existing state-of-the-art models Fan et al. (2021); Bulat et al. (2021) still require 400-1000 GFLOPs to achieve high accuracy on the Kinetics dataset Carreira & Zisserman (2017). The main result of this paper is a video recognition model that can achieve similar accuracy while *requiring* $\sim 3 - 4 \times$ *less* FLOPs (see also Fig. 1).

Specifically, and following the tremendous success of Transformers in NLP, Vaswani et al. (2017); Chen et al. (2018), the current state-of-the-art in video recognition is based on video transformers Bertasius et al. (2021); Arnab et al. (2021); Fan et al. (2021); Bulat et al. (2021). While such models have achieved significantly higher accuracy compared to traditional CNN-based approaches (*e.g.* SlowFast Feichtenhofer et al. (2019), TSM Lin et al. (2019)), they still require very large video

¹This is further exacerbated by the multi-cropping inference process, a typical process in evaluating video recognition models.

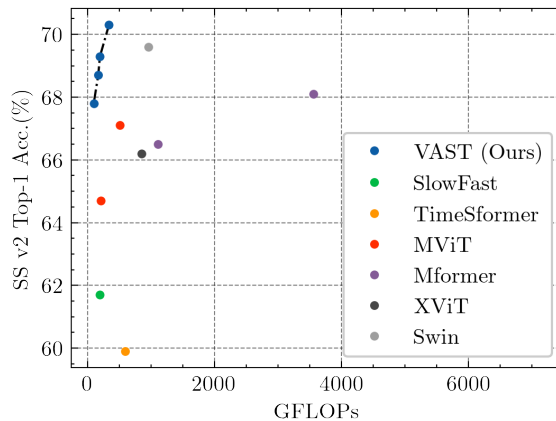


Figure 1: Our approach consistently outperforms all prior state-of-the-art in terms of efficiency-accuracy trade-off on the Something-Something-v2 dataset.

backbones to achieve these results, *e.g.* ViT-L/H in Arnab et al. (2021). In fact, the main reason that these models have dominated the accuracy-FLOPs spectrum is because they require significantly fewer number of crops during inference compared to CNN-based approaches.

Concurrently to the development of the aforementioned video transformers, there has been an independent line of research which questions the necessity of the self-attention layers in the vision transformer’s architecture. Such “attention-free” methods have proposed the use of simpler schemes based on MLPs Touvron et al. (2021a); Chen et al. (2021); Tolstikhin et al. (2021) and/or the shift operator Yu et al. (2021b; 2022) for achieving the token mixing effect akin to the self-attention layer. However, these methods have been developed for the image domain, where the cost of the self-attention is relatively low compared to the video domain, where some approximation of the full MHSA is typically necessary. As a result, these methods have not been conclusively shown to outperform self-attention-based transformers for image recognition. Moreover, there are no attention-free methods yet for the case of the video domain where the self-attention operation induces significantly higher computational and memory cost. Hence, the question we wish to address in this paper is: “*Can we construct high performing video transformers without attention?*”

To address the above question, **we make the following contributions:**

1. We introduce a new block for attention-free transformers based on the *shift operator* which is tailored to achieve high accuracy with low computational and memory footprint. Our block, coined *Affine-Shift* block and shown in Fig. 2, is specifically designed to *approximate* as closely as possible *the operations* in the MHSA block of a Transformer layer.
2. Based on our Affine-Shift block, we construct our Affine-Shift Transformer (AST). We exhaustively ablate AST in the image domain for ImageNet classification where we show that it significantly outperforms previous work particularly for the case of low complexity models.
3. By extending our Affine-Shift block in the video domain, we build a new backbone for video recognition, the proposed Video Affine-Shift Transformer (VAST). VAST has two main features: (a) it is attention-free, and (b) is purely shift-based, effectively applying, for the first time, the shift operation in *both space & time* to achieve token mixing.
4. We further evaluate VAST on multiple action recognition datasets, namely Kinetics Carreira & Zisserman (2017), Something-Something-v2 Goyal et al. (2017) and Epic Kitchens Damen et al. (2018) where we show that it can achieve similar accuracy to state-of-the-art video transformers, namely Fan et al. (2021) and Bulat et al. (2021), while *requiring* $\sim 3 - 4\times$ less FLOPs.

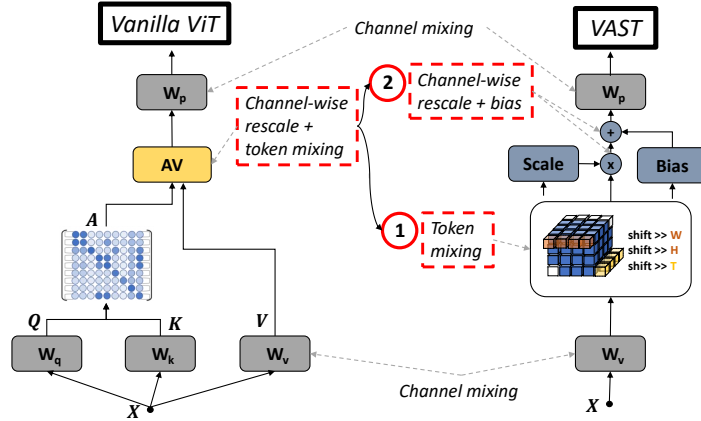


Figure 2: The proposed Affine-Shift block used to construct AST and VAST (right) and the ViT attention module (left). Our goal is to approximate as closely as possible the MHSA operations within a Transformer block: channel-wise rescaling and token mixing implemented by AV in MHSA (see also Eq. 3) are now replaced by (1) local token mixing using the shift operator followed by (2) channel-wise rescaling (using SE-like MLP) and bias correction (using DWConv). All the above mentioned steps are needed to obtain a highly accurate block/architecture.

2 RELATED WORK

Vision Transformers: After revolutionizing NLP Vaswani et al. (2017); Raffel et al. (2019), ViT Dosovitskiy et al. (2020) is the first convolution-free transformer that was shown to achieve promising results on ImageNet Deng et al. (2009). Following ViT, a number of notable extensions have been proposed Touvron et al. (2021b); Liu et al. (2021b); Wang et al. (2021b); Chu et al. (2021); Fan et al. (2021). DeiT Touvron et al. (2021b) proposes a teacher-student scheme which uses a distillation token so that the student learns from the teacher through attention. PVT Wang et al. (2021b) and MViT Fan et al. (2021) propose to compute the attention with a sub-sampled version of the input tokens. Swin Liu et al. (2021b) introduces non-overlapping local windows for computing the attention and uses a shifted window operation to increase the receptive field. Twins Chu et al. (2021) extends PVT in a number of ways emphasizing the importance of using relative positional encodings Shaw et al. (2018).

Attention-free Transformers: Very recently, the necessity of the self-attention operation within the ViT has been questioned by a number of works which propose spatial token mixing with MLPs Tolstikhin et al. (2021); Liu et al. (2021a); Touvron et al. (2021a). Moreover, such approaches have been further developed by deploying the shift operator Wu et al. (2018) and related variants for spatial token mixing giving rise to a number of recently proposed methods Lian et al. (2021); Chen et al. (2021); Yu et al. (2021b; 2022); Hou et al. (2022) which are more flexible by allowing the processing of images of different resolutions. AS-MLP Lian et al. (2021) proposes an axial shifting strategy where features are spatially shifted in both horizontal and vertical directions. CycleMLP Chen et al. (2021) applies the shift operator in a cyclical fashion along the channel dimension. S^2 -MLP Yu et al. (2022) groups channels together, and shifts each of these groups in a different direction. S^2 -MLPv2 Yu et al. (2021b) extends S^2 -MLP by expanding the channel dimension before shifting and applying a hierarchical pyramid architecture. ViP Hou et al. (2022) proposes to permute the height and the width dimension with the channel dimension.

The above works have proposed attention-free architectures in the image domain where the impact of the self-attention operations on the total computational complexity is limited. Hence, the advantage of such architectures over attention-based in terms of efficiency has not been conclusively demonstrated. In *our work*, we firstly propose the Affine-Shift Transformer (AST), which already outperforms all the above methods in the image domain. Then, we propose to extend it to build the Video Affine-Shift Transformer (VAST), the very first attention-free video transformer which sig-

nificantly outperforms attention-based video transformers, especially for the case of low complexity and memory models.

Video recognition: Video recognition has been tackled over the last years using 2D+time Wang et al. (2018); Lin et al. (2019); Liu et al. (2020) and 3D CNN-based Tran et al. (2015); Carreira & Zisserman (2017); Feichtenhofer et al. (2019) approaches. While the later are characterised by high accuracy thanks to learning strong spatio-temporal models via 3D convolutions, they yield significant computational and memory costs. Somewhere in between are 2D+time works, namely TSM and TAM Lin et al. (2019); Liu et al. (2020), that use the shift operator Wu et al. (2018) for learning a temporal model at a layer level while still relying on 2D convs.

More recently, a number of video transformers Bertasius et al. (2021); Arnab et al. (2021); Fan et al. (2021); Bulat et al. (2021), extending ViT into the video domain were proposed. The main goal of these works has been primarily to reduce the cost of the full space-time attention, which is particularly memory and computationally costly, by using spatio-temporal factorization Bertasius et al. (2021); Arnab et al. (2021), low resolution self-attention and hierarchical pyramid architecture Fan et al. (2021) and space-time mixing attention Bulat et al. (2021).

Closely related works: From the above methods, *our work* is mostly related to Lin et al. (2019); Bulat et al. (2021). Lin et al. (2019) uses the shift operator (Wu et al., 2018) for mixing channels across time while still relying on 2D convs. Bulat et al. (2021) proposes an efficient approximation to the full space-time attention using the shift operator. Therefore, Lin et al. (2019) and Bulat et al. (2021) rely on spatial convolutions and spatial attention, respectively, for processing information in the spatial domain. We go one step beyond and propose VAST which is, to the best of our knowledge, the first video transformer based purely on the shift operator for both space & time processing, further showing significant computational and memory savings without compromising accuracy.

3 METHOD

3.1 AFFINE-SHIFT & VIDEO AFFINE-SHIFT BLOCK

Transformer block: The basic building blocks of the Transformer Vaswani et al. (2017) consist of a Multi-Head Self-Attention (MHSA) layer followed by an MLP (with skip connections around them). For any transformer’s layer l , they take the form:

$$\mathbf{Y}^l = \text{MHSA}(\text{LN}(\mathbf{X}^{l-1})) + \mathbf{X}^{l-1}, \quad (1)$$

$$\mathbf{X}^l = \text{MLP}(\text{LN}(\mathbf{Y}^l)) + \mathbf{Y}^l. \quad (2)$$

where $\mathbf{X}^{l-1} \in \mathcal{R}^{S \times d}$ are the input features at layer l , $\text{LN}(\cdot)$ is the Layer Norm Ba et al. (2016) and the Self-Attention for a single head is given by:

$$\mathbf{y}_s^l = \sum_{s'=0}^{S-1} \sigma\left(\frac{\mathbf{q}_s^l \cdot \mathbf{k}_{s'}^l}{\sqrt{d_h}}\right) \mathbf{v}_{s'}^l, \quad s = 0, \dots, S-1 \quad (3)$$

where $\sigma(\cdot)$ is the `softmax` function, S is the total number of spatial locations, and $\mathbf{q}_s^l, \mathbf{k}_s^l, \mathbf{v}_s^l \in \mathbb{R}^{d_h}$ are the query, key, and value vectors computed from the input features using $\mathbf{W}_q, \mathbf{W}_k, \mathbf{W}_v \in \mathbb{R}^{d \times d_h}$. The final output is obtained by concatenating and projecting the heads using $\mathbf{W}_h \in \mathbb{R}^{d \times d}$ ($d = h d_h$).

We would like to note here that the MLP layers mix channel-wise information within each token, *i.e.* act independently on each token. Instead, the mixing of information *between* tokens, *i.e.* the mixing across spatial dimensions, is exclusively carried out by the MHSA module. Our aim is to find an effective and efficient alternative to the MHSA, *i.e.* to the token mixing component of Eq. 3.

Shift operator: Our goal is to replace the MHSA with an attention-free alternative. One direction that showed promising results as an alternative to convolutions is channel mixing using the shift operator Wu et al. (2018). The main idea is to perform data-mixing by shifting a fixed amount of channels in different directions, such that each feature vector will now contain features from adjacent locations. Note that here the term “directions” depends on the nature of the data (*i.e.* for

images it can mean up/down, left/right, for videos backward/forward etc.). We will denote with $\text{Shift}(\mathbf{X}, p, b)$ the shifting of p channels from feature tensor \mathbf{X} across dimensions $b \in \mathbb{N}$.

Affine-Shift block: Our goal is to design an attention-free transformer block, using the shift operator, which approximates as closely as possible the original transformer block. As there is no attention, there is no need to compute queries and values but we will still keep the projection matrix \mathbf{W}_v to compute the values \mathbf{V}^l from input features \mathbf{X}^{l-1} , *i.e.*, $\mathbf{V}^l = \text{LN}(\mathbf{X}^{l-1})\mathbf{W}_v$.

A naive approach would be to replace Eq. 3 with the $\text{Shift}(\cdot)$ operator, and note b_h and b_w as the width and height dimension indexes:

$$\mathbf{Z}^l = \text{Shift}(\mathbf{V}^l, p, [b_h, b_w]), \quad (4)$$

Although this works, as Table 2 shows, it is not sufficient to obtain high accuracy. While the shift operator mixes information across adjacent tokens, the signal is simply mixed but there is no scale or bias adjustment. However, as Eq. 3 shows, in self-attention, the value vectors \mathbf{v}_s^l are scaled by the attention. Moreover, each channel in the output vector \mathbf{y}_s^l is a linear combination of the corresponding channel of the value vectors, suggesting a channel-wise operation.

None of these appear so far in the formulation, suggesting that an extra (channel-wise) operation is missing. To address this, we introduce an Affine-Shift operator, that uses a small MLP to compute a channel-wise rescaling, similar to SE-net Hu et al. (2018), and a DWConv to compute a channel-wise bias. Notably, the scale factor and bias are computed from data in a dynamic manner (similar to the dynamic nature of the Transformer block). Moreover, both the MLP and the DWConv take as input the signal *post-shifting* (as also expected from the Transformer block). The proposed Affine-Shift operation is defined as:

$$\mathbf{Z}^l = \text{Shift}(\mathbf{V}^l, p, [b_h, b_w]), \quad (5)$$

$$\hat{\mathbf{Z}}^l = \mathbf{Z}^l \odot \sigma(\text{MLP}(\text{AVG}(\mathbf{Z}^l))) + \text{DWConv}(\mathbf{Z}^l), \quad (6)$$

$$\mathbf{Y}^l = \hat{\mathbf{Z}}^l \mathbf{W}_h + \mathbf{X}^{l-1} \quad (7)$$

where \odot is the Hadamard product, AVG a global average pooling layer and σ the Sigmoid function. Note that both the MLP and 3×3 DWConv layer introduce minimal computational overhead. Note that a final linear layer using \mathbf{W}_h is applied as in the original Transformer block.

Putting everything together, the proposed Affine-Shift block firstly applies \mathbf{W}_v to obtain the values by mixing the channels, then the Affine-Shift block to mix tokens and rescale & add bias channel-wise, and finally another projection \mathbf{W}_h to mix again the channels. The block is shown in Fig. 2. Note that *all the above mentioned steps* are needed to obtain a highly accurate block/architecture. See Table 2 from Section 5.

Video Affine-Shift: For video data, we have to mix information across one extra dimension (*i.e.* time), its index being noted as b_t . To accommodate this, we can naturally extend the shift operator, described in Eq. 5, as follows:

$$\mathbf{Z}^l = \text{Shift}(\mathbf{V}^l, p, [b_t, b_h, b_w]), \quad (8)$$

Effectively, instead of shifting across the last two dimensions (height and width), we shift across all three: time, height, width. Note that unless otherwise specified, the shift is applied uniformly in each (of the 3) direction. We select 1/6 channels for each direction, for a total of 1/2 channels. Both the MLP and the 2D DWConv used to compute a dynamic scale and bias are kept as is.

3.2 AST & VAST ARCHITECTURES

Using the Affine-Shift block and its video extension, we construct the Affine-Shift Transformer (AST), and the Video Affine-Shift Transformer (VAST). We follow the standard hierarchical (pyramidal) structure for our attention-free transformers, where the resolution is dropped between stages, similar to a ResNet He et al. (2016); Liu et al. (2021b); Fan et al. (2021). In all cases we use an overlapping patch embedding across space. For the time dimension the decision to enable overlaps is taken on a case-by-case basis.

For image classification (*i.e.* ImageNet), the final predictions are obtained by taking the mean across all tokens and then feeding the obtained feature to a linear classifier. Similarly, for videos, we either

Stage	Output Size	VAST-Tiny	VAST-Small	VAST-Medium
I	$\frac{H}{4} \times \frac{W}{4}$	$C_1 = 64$		
		$E_1 = 8 \times 3$	$E_1 = 8 \times 3$	$E_1 = 8 \times 3$
II	$\frac{H}{8} \times \frac{W}{8}$	$C_2 = 128$		
		$E_2 = 8 \times 4$	$E_2 = 8 \times 4$	$E_2 = 8 \times 8$
III	$\frac{H}{16} \times \frac{W}{16}$	$C_3 = 320$		
		$E_3 = 4 \times 8$	$E_3 = 4 \times 22$	$E_3 = 4 \times 33$
IV	$\frac{H}{32} \times \frac{W}{32}$	$C_4 = 512$		
		$E_4 = 4 \times 3$	$E_4 = 4 \times 3$	$E_4 = 4 \times 3$

Table 1: Model definitions for the proposed AST and VAST. E_i defines the expansion rate at each stage inside the MLP while the multiplier the number of blocks at the current stage. C_i denotes the number of channels. T is kept constant across stages.

form a feature representation via global pooling or aggregate the data using the temporal attention aggregation layer proposed in Arnab et al. (2021); Bulat et al. (2021) before passing it to a classifier.

To differentiate between the variants of our model, we align our nomenclature to that of Dosovitskiy et al. (2020) and detail the exact configurations in Table 1.

4 EXPERIMENTAL DETAILS

Datasets: We trained and evaluated our models for large-scale image recognition on ImageNet Deng et al. (2009), and on 4 action recognition datasets, namely on Kinetics-400 and Kinetics-600 Kay et al. (2017), Something-Something-v2 Goyal et al. (2017) and Epic Kitchens-100 Damen et al. (2020). ImageNet experiments aim to confirm the effectiveness of the proposed AST compared to other recently proposed shift-based and MLP-based architectures *as these works have not been applied to video domain before*. See supplementary material for a description of the datasets.

Training details on Video: All models, unless otherwise stated, were trained following Fan et al. (2021): specifically, our models were trained using AdamW Loshchilov & Hutter (2017) with cosine scheduler Loshchilov & Hutter (2016) and linear warmup for a total of 50 epochs. The base learning rate, set at a batch size of 128, was $2e - 4$ ($4e - 4$ for SSv2) and weight decay was 0.05. To prevent over-fitting we made use of the following augmentation techniques: random scaling ($0.08 \times$ to $1.0 \times$) and cropping, random flipping (with probability of 0.5; not for SSv2), rand augment Cubuk et al. (2020), color jitter (0.4), mixup ($\alpha = 0.8$) Zhang et al. (2018) and cutmix ($\alpha = 1$) Yun et al. (2019), random erasing Zhong et al. (2020) and label smoothing ($\lambda = 0.1$) Szegedy et al. (2016). During training with a 50% probability we chose between cutmix and mixup. All augmentations are applied consistently across each frame to prevent the introduction of temporal distortions. For Kinetics we set the path dropout rate to 0.1 while on SSv2 to 0.3.

The models were initialised from models pre-trained on ImageNet-1k for Kinetics-400/600 and from Kinetics-400 on Something-Something-v2. When initialising from a 2D model, if a 3D patch embedding is used, we initialized it using the strategy from Fan et al. (2021). We only use a 3D patch embedding for SSv2. The models were trained on 8 V100 GPUs using PyTorch Paszke et al. (2019).

Testing details on Video: Unless otherwise stated, we used 8, 16 or 32 frames. Note that when a 3D stem is used (*i.e.* on SSv2), the effective temporal dimension is halved. We report results for 1×3 views (1 temporal clip and 3 spatial crops) following Bertasius et al. (2021); Bulat et al. (2021).

5 ABLATION STUDIES

5.1 AFFINE SHIFT ANALYSIS AND VARIATIONS

Firstly we analyse the impact of the three main components described in the Affine-Shift module: the shift operation, the dynamical re-scaling (MLP) and the bias (DWC_{CONV}) in Eq. 6. As Table 2

shows, replacing the MHSA with `Shift(.)` (R1) works reasonable well and sets a strong baseline result. Adding the dynamic bias (R2) and scale (R3) on their own improves the result in each case by almost 1.5%. Finally, combining the 3 components together (R4) produces the strongest result. This showcases that all of the introduced components are necessary.

The transformer block consists of MHSA and MLP blocks (Eq. 1- 2). As we already replaced the MHSA with `Shift(.)`, a natural question to ask is whether we can further improve the results by adding an additional shift within the MLP block in the transformer. As the results show (R5), the performance saturates and no additional gains are observed. This suggests that due to the number of layers, the effective receptive size toward the end of the network is sufficiently large to cover the entire image making additional shift operations redundant.

Block variant	Top-1%
(R1) ours - w/o scale & w/o bias	79.4
(R2) ours - w/o scale	80.7
(R3) ours - w/o bias	80.9
(R4) ours	81.8
(R5) ours + extra shift	81.7
(R6) only shift	79.0

Table 2: Effect of various shift-based variants of our method in terms of Top-1 accuracy (%) on ImageNet. See Section 5.1 for details. All models have roughly 3.9 GFLOPs.

A perhaps overlooked detail is the placement of the drop-path. Normally drop-path randomly drops the MHSA and/or the MLP block at train time. However, by-passing an Affine-Shift block will result in skipping a data mixing step, effectively producing information with slightly different spatial, temporal, or spatio-temporal context. As such for all of our model, we remove the path drop that affects our Affine-Shift block. Finally, we compare our approach with a more direct alternative, that of replacing Eq. 1 in its entirety with a shift operation. As the results show (R6), while promising, the Affine-Shift block is significantly better.

5.2 HOW MANY CHANNELS SHOULD WE SHIFT?

A potentially important factor that could influence the accuracy of the network is the total amount of channels shifted across all dimensions. As the results from Table 3 show, the proposed module is generally robust to the amount of shift within the range 25% – 50%. We note that sustaining the accuracy at lower levels of shift is especially promising for video data, where the number of dimensions we need to shift across increases.

	0%	25%	33%	50%
% channels shift	60.2	81.5	81.8	81.7

Table 3: Impact of the number of shifted channels on the overall accuracy in terms of Top-1 acc (%) on ImageNet.

6 COMPARISON TO STATE-OF-THE-ART

6.1 IMAGENET-1K

In Table 4, we report results on ImageNet for the variant of most interest - tiny (AST-Ti) of our model. Moreover, we report the results of all recently proposed Shift/MLP- and MLP-based backbones. As it can be observed, our tiny model, AST-Ti, is the most accurate among models of similar size with only Cycle-MLP-B2 closely following. Further results and comparison for models sizes: small (AST-S) and medium (AST-B) are reported in the supplementary material.

Note that our goal is not highly-accurate image recognition using very big models but efficient video recognition and hence we did not train or evaluate very big image models. The results of Table 4 clearly show that our model is already a very good candidate for highly accurate and efficient video recognition, outperforming all other Shift/MLP- and MLP-based approaches.

Arch.	Method	#Param FLOPs		Train Size	Test Size	ImageNet Top-1
		(M)	(G)			
Trans	DeiT-S (Touvron et al., 2021b)	22	4.6	224	224	79.9
	PVTv2-B2-Li (Wang et al., 2021a)	25	3.9	224	224	82.1
	Swin-T (Liu et al., 2021b)	29	4.5	224	224	81.3
	Focal-T (Yang et al., 2021)	29	4.9	224	224	82.2
Hyb.	CvT-13 (Wu et al., 2021)	20	4.5	224	224	81.6
	CoAtNet-0 (Dai et al., 2021)	25	4.2	224	224	81.6
	LV-ViT-S (Jiang et al., 2021)	26	6.6	224	224	83.3
No-attn.	EAMLP-14 (Guo et al., 2021)	30	—	224	224	78.9
	ResMLP-S24 (Touvron et al., 2021a)	30	6.0	224	224	79.4
	gMLP-S (Liu et al., 2021a)	20	4.5	224	224	79.6
	GFNet-S (Rao et al., 2021)	25	4.5	224	224	80.0
	GFNet-H-S (Rao et al., 2021)	32	4.5	224	224	81.5
	AS-MLP-T (Lian et al., 2021)	28	4.4	224	224	81.3
	CycleMLP-B2 (Chen et al., 2021)	27	3.9	224	224	81.6
	ViP-Small/7 (Hou et al., 2022)	25	6.9	224	224	81.5
	S ² -MLPv2-Small/7 (Yu et al., 2021b)	25	6.9	224	224	82.0
	AST-Ti (Ours)	19	3.9	224	224	81.8

Table 4: **Comparisons on ImageNet.** Our models are the most accurate within the “No. attn.” category. Hyb. = CNN+Transformer.

Method	Pre-train	Top-1 Acc. (%)	Top-5 Acc. (%)	Frames	Views	FLOPs $\times 10^9$
CNN models						
SlowFast (Feichtenhofer et al., 2019)	K-400	61.7	-	8	1 \times 3	197
TSM (R50) (Lin et al., 2019)	K-400	63.3	88.5	16	2 \times 3	650
MSNet (Kwon et al., 2020)	IN-1k	64.7	89.4	16	-	-
TEA (Li et al., 2020)	IN-1k	65.1	89.9	16	10 \times 3	2,100
bLVNet (Fan et al., 2019)	IN-1k	65.2	90.3	32	10 \times 3	3,870
CT-Net (Li et al., 2021)	IN-1k	65.9	90.1	16	2 \times 3	450
TAdaConvNeXt-T (Huang et al., 2022)	K400	67.1	90.4	32	2 \times 3	564
Transformer and Hybrid models						
TimeSformer (Bertasius et al., 2021)	IN-21k	59.5	-	96	1 \times 3	590
TimeSformer-L (Bertasius et al., 2021)	IN-21k	62.4	-	96	1 \times 3	7,140
ViViT-L/16x2 (Arnab et al., 2021)	IN-21k+K-400	65.4	89.8	32	4 \times 3	17,352
XViT-B (Bulat et al., 2021)	IN-21k	66.2	90.6	16	1 \times 3	850
XViT-B (Bulat et al., 2021)	K-600	67.2	90.8	16	1 \times 3	850
MViT-B (16 \times 4) (Fan et al., 2021)	K-400	64.7	89.2	16	1 \times 3	211
MViT-B (32 \times 4) (Fan et al., 2021)	K-600	67.8	91.3	16	1 \times 3	510
Mformer (Patrick et al., 2021)	IN-21k+K-400	66.5	90.1	-	1 \times 3	1,110
Mformer-HR (Patrick et al., 2021)	IN-21k+K-400	68.1	90.8	-	1 \times 3	3,555
Swin-B (Liu et al., 2021c)	IN-21k+K-400	69.6	92.7	-	1 \times 3	963
MLP models (Attention-free transformers)						
VAST-Ti (Ours)	K-400	67.8	90.8	16	1 \times 3	98
VAST-Ti (Ours)	K-400	69.3	91.3	32	1 \times 3	196
VAST-S (Ours)	K-400	68.7	91.0	16	1 \times 3	169
VAST-S (Ours)	K-400	70.9	92.1	32	1 \times 3	338

Table 5: Comparison with CNN-based methods and state-of-the-art video transformers on Something-Something-v2. Our tiniest model VAST-Ti-8 largely outperforms the lightest MViT (+2%) while utilizing 2 \times fewer FLOPs, and it is only 0.4% behind than the lightest XViT while utilizing less than 4 \times fewer FLOPs. Larger models show improved accuracy inducing only modest computational overheads, outperforming prior results by a large margin.

6.2 VIDEO ACTION RECOGNITION

We report the accuracy achieved by 4 different variants of our models: tiny and small for both 8 and 16 frames, that is VAST-Ti-8, VAST-Ti-16 & VAST-S-8, VAST-S-16. Our models were initialized

Method	Pre-train	Top-1 Acc. (%)	Top-5 Acc. (%)	Frames	Views	FLOPs $\times 10^9$
CNN models						
TSM (R50) (Lin et al., 2019)	IN-1k	74.7	-	16	10×3	650
SlowFast (Feichtenhofer et al., 2019)	-	78.7	93.5	8	10×3	3,480
X3D-S (Feichtenhofer, 2020)	-	72.9	90.5	-	10×3	58
X3D-XXL (Feichtenhofer, 2020)	-	80.4	94.6	-	10×3	5,823
TAdaConvNeXt-T (Huang et al., 2022)	IN-1K	79.1	93.7	32	4×3	1,128
Transformer and hybrid models						
TimeSformer (Bertasius et al., 2021)	IN-1k	75.8	-	8	1×3	590
TimeSformer (Bertasius et al., 2021)	IN-21k	78.0	93.7	8	1×3	590
TimeSformer-L (Bertasius et al., 2021)	IN-21k	80.7	94.7	96	1×3	7,140
ViViT-B/16x2 (Arnab et al., 2021)	IN-21k	78.8	-	32	4×3	3,408
ViViT-L/16x2 (Arnab et al., 2021)	IN-21k	80.6	94.7	32	4×3	17,352
Mformer (Patrick et al., 2021)	IN-21k	79.7	94.2	-	10×3	11,070
Mformer-HR Patrick et al. (2021)	IN-21k	81.1	95.2	-	10×3	28,764
XViT-B (Bulat et al., 2021)	IN-21k	78.4	93.7	8	1×3	425
XViT-B (Bulat et al., 2021)	IN-21k	80.2	94.7	16	1×3	850
MViT-S (Fan et al., 2021)	-	76.0	92.1	-	1×5	165
MViT-B (16×4) (Fan et al., 2021)	-	78.4	93.5	16	1×5	352
MViT-B (64×3) (Fan et al., 2021)	-	81.2	95.1	64	3×3	4,095
En-VidTr-S (Zhang et al., 2021)	IN-21k	79.4	94.0	8	10×3	3,900
En-VidTr-M (Zhang et al., 2021)	IN-21k	79.7	94.2	16	10×3	6,600
En-VidTr-L (Zhang et al., 2021)	IN-21k	80.5	94.6	32	10×3	11,760
Swin-T (Liu et al., 2021c)	IN-1k	78.8	93.6	-	4×3	1,056
Swin-S (Liu et al., 2021c)	IN-1k	80.6	94.5	-	4×3	1,992
Swin-L (384) (Liu et al., 2021c)	IN-21k	84.9	96.7	-	10×5	105,350
MLP models (Attention-free transformers)						
VAST-Ti (Ours)	IN-1k	78.0	93.2	8	1×3	98
VAST-Ti (Ours)	IN-1k	79.0	93.8	16	1×3	196
VAST-S (Ours)	IN-1k	78.9	93.8	8	1×3	169
VAST-S (Ours)	IN-1k	80.0	94.5	16	1×3	338

Table 6: Comparison with CNN-based methods and state-of-the-art video transformers on Kinetics-400. Our tiniest model VAST-Ti-8 largely outperforms the lightest MViT (+2%) while utilizing $2 \times$ fewer FLOPs, and it is only 0.4% behind than the lightest XViT while utilizing less than $4 \times$ fewer FLOPs. Our biggest model VAST-S-16 matches the best XViT model while utilizing less than $2 \times$ fewer FLOPs.

with ImageNet-1K pre-training for K-400 and K-600, while for SSv2 we used the models trained on K-400. For SSv2, we use a 3D stem, reducing the temporal dimensionality by 2. Thus, if for example we note 32 input frames, the actual configuration (and cost) corresponds to the 16-frame VAST variants.

We compare with the state-of-the-art in video recognition: In addition to classic CNN-based approaches, we compare against early attempts in video transformers, namely TimeSformer Bertasius et al. (2021), ViVit Arnab et al. (2021) and VidTr Zhang et al. (2021), Mformer Patrick et al. (2021), the video version of the Swin Transformer Liu et al. (2021c) as well as the state-of-the-art, namely MViT Fan et al. (2021) and XViT Bulat et al. (2021). For all of these models, we have included both light and heavy versions.

K-400 & K-600: Table 6 shows our results on **K-400**. It can be seen that our tiny model VAST-Ti-8 largely outperforms all early approaches to video transformers (Bertasius et al., 2021; Arnab et al., 2021; Patrick et al., 2021; Liu et al., 2021c), as well as the lightest version of MViT (+2%) while utilizing $2 \times$ fewer FLOPs, and it is only 0.4% behind the most efficient version of XViT (initialized in ImageNet-21K) while utilizing less than $4 \times$ fewer FLOPs. Moreover, our larger models show improved accuracy, inducing only modest computational overheads. Our biggest model VAST-S-16 matches the best XViT model while utilizing less than $2 \times$ fewer FLOPs. See supplementary material for results on **K-600**, where we draw similar conclusions.

It is worth noting that XViT uses an efficient local space-time attention also based on the shift operator. Our results show that our purely shift-based model is significantly more efficient (in terms

of accuracy vs FLOPs) without using any attention layers at all.

SSv2: On **SSv2**, we firstly emphasize that initialization plays a very important role and that models initialized on different dataset are hard to compare. In light of this, and since we pre-trained our models on K-400, only comparisons with methods pre-trained there (and potentially on K-600) are meaningful. As Table 5 shows, our models significantly outperform all other models in terms of accuracy vs FLOPs. For example, our lightest model (VAST-Ti) outperforms the lightest XViT and MViT by 3.4% and 3.1% while utilizing less than $4\times$ and $2\times$ fewer FLOPs, respectively. Again, our larger models show significant accuracy improvements inducing only modest computational overheads, outperforming other models by large margin.

Epic-100: Similar conclusions can be drawn by observing our results on **Epic-100**; see supplementary material.

7 CONCLUSIONS

In the paper’s introduction we posed the question “can we construct high performing video transformers without attention?” The results provided in our results section clearly demonstrated that the answer to this question is positive. To this end, we introduced a new purely shift-based block coined *Affine-Shift*, specifically designed to *approximate* as closely as possible *the operations* in the MHSA block of a Transformer layer. Based on our Affine-Shift block, we constructed AST and show that it outperforms previous work particularly for the case of low complexity models. By extending our Affine-Shift block in the video domain, we built VAST and then showed that it is significantly more efficient than existing state-of-the-art video transformers.

REFERENCES

- Anurag Arnab, Mostafa Dehghani, Georg Heigold, Chen Sun, Mario Lučić, and Cordelia Schmid. Vivit: A video vision transformer. *arXiv preprint arXiv:2103.15691*, 2021.
- Jimmy Lei Ba, Jamie Ryan Kiros, and Geoffrey E Hinton. Layer normalization. *arXiv preprint arXiv:1607.06450*, 2016.
- Gedas Bertasius, Heng Wang, and Lorenzo Torresani. Is space-time attention all you need for video understanding? *arXiv preprint arXiv:2102.05095*, 2021.
- Adrian Bulat, Juan Manuel Perez Rúa, Swathikiran Sudhakaran, Brais Martinez, and Georgios Tzimiropoulos. Space-time mixing attention for video transformer. *NeurIPS*, 2021.
- Joao Carreira and Andrew Zisserman. Quo vadis, action recognition? a new model and the kinetics dataset. In *CVPR*, 2017.
- Mia Xu Chen, Orhan Firat, Ankur Bapna, Melvin Johnson, Wolfgang Macherey, George Foster, Llion Jones, Niki Parmar, Mike Schuster, Zhifeng Chen, et al. The best of both worlds: Combining recent advances in neural machine translation. *arXiv preprint arXiv:1804.09849*, 2018.
- Shoufa Chen, Enze Xie, Chongjian Ge, Ding Liang, and Ping Luo. Cyclemlp: A mlp-like architecture for dense prediction. *arXiv preprint arXiv:2107.10224*, 2021.
- Xiangxiang Chu, Zhi Tian, Yuqing Wang, Bo Zhang, Haibing Ren, Xiaolin Wei, Huaxia Xia, and Chunhua Shen. Twins: Revisiting the design of spatial attention in vision transformers. *NeurIPS*, 2021.
- Ekin D Cubuk, Barret Zoph, Jonathon Shlens, and Quoc V Le. Randaugment: Practical automated data augmentation with a reduced search space. In *Proceedings of the IEEE/CVF Conference on Computer Vision and Pattern Recognition Workshops*, pp. 702–703, 2020.
- Zihang Dai, Hanxiao Liu, Quoc Le, and Mingxing Tan. Coatnet: Marrying convolution and attention for all data sizes. *Advances in Neural Information Processing Systems*, 34, 2021.

-
- Dima Damen, Hazel Doughty, Giovanni Maria Farinella, Sanja Fidler, Antonino Furnari, Evangelos Kazakos, Davide Moltisanti, Jonathan Munro, Toby Perrett, Will Price, et al. Scaling egocentric vision: The epic-kitchens dataset. In *ECCV*, 2018.
- Dima Damen, Hazel Doughty, Giovanni Maria Farinella, Antonino Furnari, Evangelos Kazakos, Jian Ma, Davide Moltisanti, Jonathan Munro, Toby Perrett, Will Price, et al. Rescaling egocentric vision. *arXiv preprint arXiv:2006.13256*, 2020.
- Jia Deng, Wei Dong, Richard Socher, Li-Jia Li, Kai Li, and Li Fei-Fei. Imagenet: A large-scale hierarchical image database. In *CVPR*, 2009.
- Alexey Dosovitskiy, Lucas Beyer, Alexander Kolesnikov, Dirk Weissenborn, Xiaohua Zhai, Thomas Unterthiner, Mostafa Dehghani, Matthias Minderer, Georg Heigold, Sylvain Gelly, et al. An image is worth 16x16 words: Transformers for image recognition at scale. *arXiv preprint arXiv:2010.11929*, 2020.
- Haoqi Fan, Bo Xiong, Karttikeya Mangalam, Yanghao Li, Zhicheng Yan, Jitendra Malik, and Christoph Feichtenhofer. Multiscale vision transformers. *arXiv preprint arXiv:2104.11227*, 2021.
- Quanfu Fan, Chun-Fu Chen, Hilde Kuehne, Marco Pistoia, and David Cox. More is less: Learning efficient video representations by big-little network and depthwise temporal aggregation. *arXiv preprint arXiv:1912.00869*, 2019.
- Christoph Feichtenhofer. X3d: Expanding architectures for efficient video recognition. In *CVPR*, 2020.
- Christoph Feichtenhofer, Haoqi Fan, Jitendra Malik, and Kaiming He. Slowfast networks for video recognition. In *ICCV*, 2019.
- Raghav Goyal, Samira Ebrahimi Kahou, Vincent Michalski, Joanna Materzynska, Susanne Westphal, Heuna Kim, Valentin Haenel, Ingo Fruend, Peter Yianilos, Moritz Mueller-Freitag, et al. The” something something” video database for learning and evaluating visual common sense. In *ICCV*, 2017.
- Meng-Hao Guo, Zheng-Ning Liu, Tai-Jiang Mu, and Shi-Min Hu. Beyond self-attention: External attention using two linear layers for visual tasks. *arXiv preprint arXiv:2105.02358*, 2021.
- Kaiming He, Xiangyu Zhang, Shaoqing Ren, and Jian Sun. Deep residual learning for image recognition. In *CVPR*, 2016.
- Qibin Hou, Zihang Jiang, Li Yuan, Ming-Ming Cheng, Shuicheng Yan, and Jiashi Feng. Vision permutator: A permutable mlp-like architecture for visual recognition. *TPAMI*, 2022.
- Jie Hu, Li Shen, and Gang Sun. Squeeze-and-excitation networks. In *CVPR*, 2018.
- Ziyuan Huang, Shiwei Zhang, Liang Pan, Zhiwu Qing, Mingqian Tang, Ziwei Liu, and Marcelo H Ang Jr. Tada! temporally-adaptive convolutions for video understanding. 2022.
- Boyuan Jiang, MengMeng Wang, Weihao Gan, Wei Wu, and Junjie Yan. Stm: Spatiotemporal and motion encoding for action recognition. In *ICCV*, 2019.
- Zi-Hang Jiang, Qibin Hou, Li Yuan, Daquan Zhou, Yujun Shi, Xiaojie Jin, Anran Wang, and Jiashi Feng. All tokens matter: Token labeling for training better vision transformers. *Advances in Neural Information Processing Systems*, 34, 2021.
- Will Kay, Joao Carreira, Karen Simonyan, Brian Zhang, Chloe Hillier, Sudheendra Vijayanarasimhan, Fabio Viola, Tim Green, Trevor Back, Paul Natsev, et al. The kinetics human action video dataset. *arXiv preprint arXiv:1705.06950*, 2017.
- Evangelos Kazakos, Arsha Nagrani, Andrew Zisserman, and Dima Damen. Epic-fusion: Audio-visual temporal binding for egocentric action recognition. In *ICCV*, 2019.
- Heeseung Kwon, Manjin Kim, Suha Kwak, and Minsu Cho. Motionsqueeze: Neural motion feature learning for video understanding. In *ECCV*, 2020.

-
- Kunchang Li, Xianhang Li, Yali Wang, Jun Wang, and Yu Qiao. Ct-net: Channel tensorization network for video classification. *arXiv preprint arXiv:2106.01603*, 2021.
- Yan Li, Bin Ji, Xintian Shi, Jianguo Zhang, Bin Kang, and Limin Wang. TEA: Temporal excitation and aggregation for action recognition. In *CVPR*, 2020.
- Dongze Lian, Zehao Yu, Xing Sun, and Shenghua Gao. As-mlp: An axial shifted mlp architecture for vision. *arXiv preprint arXiv:2107.08391*, 2021.
- Ji Lin, Chuang Gan, and Song Han. Tsm: Temporal shift module for efficient video understanding. In *ICCV*, 2019.
- Hanxiao Liu, Zihang Dai, David So, and Quoc Le. Pay attention to mlps. *NeurIPS*, 2021a.
- Ze Liu, Yutong Lin, Yue Cao, Han Hu, Yixuan Wei, Zheng Zhang, Stephen Lin, and Baining Guo. Swin transformer: Hierarchical vision transformer using shifted windows. In *ICCV*, 2021b.
- Ze Liu, Jia Ning, Yue Cao, Yixuan Wei, Zheng Zhang, Stephen Lin, and Han Hu. Video swin transformer. *arXiv preprint arXiv:2106.13230*, 2021c.
- Zhaoyang Liu, Limin Wang, Wayne Wu, Chen Qian, and Tong Lu. Tam: Temporal adaptive module for video recognition. *arXiv preprint arXiv:2005.06803*, 2020.
- Ilya Loshchilov and Frank Hutter. Sgdr: Stochastic gradient descent with warm restarts. *arXiv preprint arXiv:1608.03983*, 2016.
- Ilya Loshchilov and Frank Hutter. Decoupled weight decay regularization. *arXiv preprint arXiv:1711.05101*, 2017.
- Adam Paszke, Sam Gross, Francisco Massa, Adam Lerer, James Bradbury, Gregory Chanan, Trevor Killeen, Zeming Lin, Natalia Gimelshein, Luca Antiga, et al. Pytorch: An imperative style, high-performance deep learning library. *arXiv preprint arXiv:1912.01703*, 2019.
- Mandela Patrick, Dylan Campbell, Yuki Asano, Ishan Misra, Florian Metz, Christoph Feichtenhofer, Andrea Vedaldi, and João F Henriques. Keeping your eye on the ball: Trajectory attention in video transformers. *NeurIPS*, 2021.
- Ilija Radosavovic, Raj Prateek Kosaraju, Ross Girshick, Kaiming He, and Piotr Dollár. Designing network design spaces. In *Proceedings of the IEEE/CVF Conference on Computer Vision and Pattern Recognition*, pp. 10428–10436, 2020.
- Colin Raffel, Noam Shazeer, Adam Roberts, Katherine Lee, Sharan Narang, Michael Matena, Yanqi Zhou, Wei Li, and Peter J Liu. Exploring the limits of transfer learning with a unified text-to-text transformer. *arXiv preprint arXiv:1910.10683*, 2019.
- Yongming Rao, Wenliang Zhao, Zheng Zhu, Jiwen Lu, and Jie Zhou. Global filter networks for image classification. *NeurIPS*, 2021.
- Peter Shaw, Jakob Uszkoreit, and Ashish Vaswani. Self-attention with relative position representations. *arXiv preprint arXiv:1803.02155*, 2018.
- Christian Szegedy, Vincent Vanhoucke, Sergey Ioffe, Jon Shlens, and Zbigniew Wojna. Rethinking the inception architecture for computer vision. In *CVPR*, 2016.
- Mingxing Tan and Quoc Le. Efficientnet: Rethinking model scaling for convolutional neural networks. In *International conference on machine learning*, pp. 6105–6114. PMLR, 2019.
- Mingxing Tan and Quoc Le. Efficientnetv2: Smaller models and faster training. In *International Conference on Machine Learning*, pp. 10096–10106. PMLR, 2021.
- Ilya O Tolstikhin, Neil Houlsby, Alexander Kolesnikov, Lucas Beyer, Xiaohua Zhai, Thomas Unterthiner, Jessica Yung, Andreas Steiner, Daniel Keysers, Jakob Uszkoreit, et al. Mlp-mixer: An all-mlp architecture for vision. *NeurIPS*, 2021.

-
- Hugo Touvron, Piotr Bojanowski, Mathilde Caron, Matthieu Cord, Alaaeldin El-Nouby, Edouard Grave, Gautier Izacard, Armand Joulin, Gabriel Synnaeve, Jakob Verbeek, et al. Resmlp: Feedforward networks for image classification with data-efficient training. *arXiv preprint arXiv:2105.03404*, 2021a.
- Hugo Touvron, Matthieu Cord, Matthijs Douze, Francisco Massa, Alexandre Sablayrolles, and Hervé Jégou. Training data-efficient image transformers & distillation through attention. In *ICML*, 2021b.
- Du Tran, Lubomir Bourdev, Rob Fergus, Lorenzo Torresani, and Manohar Paluri. Learning spatiotemporal features with 3d convolutional networks. In *ICCV*, 2015.
- Ashish Vaswani, Noam Shazeer, Niki Parmar, Jakob Uszkoreit, Llion Jones, Aidan N Gomez, Lukasz Kaiser, and Illia Polosukhin. Attention is all you need. *arXiv preprint arXiv:1706.03762*, 2017.
- Limin Wang, Yuanjun Xiong, Zhe Wang, Yu Qiao, Dahua Lin, Xiaoou Tang, and Luc Van Gool. Temporal segment networks for action recognition in videos. *TPAMI*, 41(11):2740–2755, 2018.
- Wenhai Wang, Enze Xie, Xiang Li, Deng-Ping Fan, Kaitao Song, Ding Liang, Tong Lu, Ping Luo, and Ling Shao. Pvtv2: Improved baselines with pyramid vision transformer. *ArXiv*, abs/2106.13797, 2021a.
- Wenhai Wang, Enze Xie, Xiang Li, Deng-Ping Fan, Kaitao Song, Ding Liang, Tong Lu, Ping Luo, and Ling Shao. Pyramid vision transformer: A versatile backbone for dense prediction without convolutions. In *ICCV*, 2021b.
- Bichen Wu, Alvin Wan, Xiangyu Yue, Peter Jin, Sicheng Zhao, Noah Golmant, Amir Gholaminejad, Joseph Gonzalez, and Kurt Keutzer. Shift: A zero flop, zero parameter alternative to spatial convolutions. In *CVPR*, 2018.
- Haiping Wu, Bin Xiao, Noel Codella, Mengchen Liu, Xiyang Dai, Lu Yuan, and Lei Zhang. Cvt: Introducing convolutions to vision transformers. In *Proceedings of the IEEE/CVF International Conference on Computer Vision*, pp. 22–31, 2021.
- Jianwei Yang, Chunyuan Li, Pengchuan Zhang, Xiyang Dai, Bin Xiao, Lu Yuan, and Jianfeng Gao. Focal self-attention for local-global interactions in vision transformers. *arXiv preprint arXiv:2107.00641*, 2021.
- Tan Yu, Xu Li, Yunfeng Cai, Mingming Sun, and Ping Li. Rethinking token-mixing MLP for mlp-based vision backbone. *BMVC*, 2021a.
- Tan Yu, Xu Li, Yunfeng Cai, Mingming Sun, and Ping Li. S2-mlpv2: Improved spatial-shift mlp architecture for vision. *arXiv preprint arXiv:2108.01072*, 2021b.
- Tan Yu, Xu Li, Yunfeng Cai, Mingming Sun, and Ping Li. S2-mlp: Spatial-shift mlp architecture for vision. In *WACV*, 2022.
- Sangdoon Yun, Dongyoon Han, Seong Joon Oh, Sanghyuk Chun, Junsuk Choe, and Youngjoon Yoo. Cutmix: Regularization strategy to train strong classifiers with localizable features. In *Proceedings of the IEEE/CVF international conference on computer vision*, pp. 6023–6032, 2019.
- Hongyi Zhang, Moustapha Cisse, Yann N Dauphin, and David Lopez-Paz. mixup: Beyond empirical risk minimization. *ICLR*, 2018.
- Yanyi Zhang, Xinyu Li, Chunhui Liu, Bing Shuai, Yi Zhu, Biagio Brattoli, Hao Chen, Ivan Marsic, and Joseph Tighe. Vidtr: Video transformer without convolutions. In *ICCV*, 2021.
- Zhun Zhong, Liang Zheng, Guoliang Kang, Shaozi Li, and Yi Yang. Random erasing data augmentation. In *AAAI*, 2020.
- Bolei Zhou, Alex Andonian, Aude Oliva, and Antonio Torralba. Temporal relational reasoning in videos. In *ECCV*, 2018.

A APPENDIX

B DATASETS

We trained and evaluated our models for large-scale image recognition on ImageNet Deng et al. (2009), and on 4 action recognition datasets, namely on Kinetics-400 and Kinetics-600 Kay et al. (2017), Something-Something-v2 Goyal et al. (2017) and Epic Kitchens-100 Damen et al. (2020). ImageNet experiments aim to confirm the effectiveness of the proposed AST compared to other recently proposed shift-based and MLP-based architectures *as these works have not been applied to video domain before*.

ImageNet: We used the standard ImageNet-1K consisting of 1.2M training images and 50K validation images belonging to 1K classes.

Kinetics-400 & 600: The Kinetics-400 (K-400) and 600 (K-600) datasets consist of pre-segmented YouTube clips, typically of duration of up to 10 seconds, labeled with 400 and 600 classes of human activities, respectively. As many of the original clips are no longer available, we used the ones made available by the CVD foundation ². Due to the nature of the data and the actions being performed, video models strongly relying on appearance-only information already perform very well on these datasets.

Something-Something-v2: The Something-Something-v2 (SSv2) dataset consists of more than 220K videos of duration between 2 and 6 seconds depicting humans performing basic actions with everyday objects. Unlike Kinetics, the dataset tends to favor models with strong temporal modeling due to the nature of the actions being performed and the fact that the objects and the backgrounds in the videos are consistent across the classes.

Epic Kitchens-100: The dataset is labeled using 97 verb classes and 300 noun classes. The evaluation results are reported using the standard action recognition protocol: the network predicts the “verb” and the “noun” using two heads. The predictions are then merged to construct an “action” which is used to report the accuracy.

C ADDITIONAL RESULTS ON EPIC KITCHENS 100

In addition to the results reported on Kinetics-400/600 and Something-Something-v2, herein we report results on the Epic Kitchens 100 dataset. As the results from Table 7 show, our method matches and outperforms significantly bigger models, pretrained on larger datasets.

²<https://github.com/cvdfoundation/kinetics-dataset>

Method	Pre-train	Action Acc. (%)	Verb Acc. (%)	Noun Acc. (%)
CNN models				
TSN (Wang et al., 2018)	IN-1k	33.2	60.2	46.0
TRN (Zhou et al., 2018)	IN-1k	35.3	65.9	44.4
TBN (Kazakos et al., 2019)	IN-1k	36.7	66.0	47.2
TSM (Lin et al., 2019)	K400	38.3	67.9	49.0
SlowFast (Feichtenhofer et al., 2019)	K400	38.5	65.6	50.0
Transformer models				
ViViT-L/16x2 (Arnab et al., 2021)	IN-21k + K400	44.0	66.4	56.8
Mformer (Patrick et al., 2021)	IN-21k + K400	43.1	66.7	56.5
Mformer-HR (Patrick et al., 2021)	IN-21k + K400	44.5	67.0	58.5
XViT-B (x8) (Bulat et al., 2021)	IN-21k + K400	41.5	66.7	53.3
XViT-B (x16) (Bulat et al., 2021)	IN-21k + K400	44.3	68.7	56.4
MLP models (Attention-free transformers)				
VAST-Ti (x8) (Ours)	K400	42.3	69.3	54.0
VAST-Ti (x16) (Ours)	K400	45.0	70.0	56.0

Table 7: Comparison with CNN-based methods and state-of-the-art video transformers on Epic Kitchens 100.

Arch.	Method	#Param (M)	FLOPs (G)	Train Size	Test Size	ImageNet Top-1
CNN	RegNetY-4G (Radosavovic et al., 2020)	21	4.0	224	224	80.0
	EfficientNet-B5 (Tan & Le, 2019)	30	9.9	456	456	83.6
	EfficientNetV2-S (Tan & Le, 2021)	22	8.5	384	384	83.9
Trans	DeiT-S (Touvron et al., 2021b)	22	4.6	224	224	79.9
	PVTv2-B2-Li (Wang et al., 2021a)	25	3.9	224	224	82.1
	Swin-T (Liu et al., 2021b)	29	4.5	224	224	81.3
	Focal-T (Yang et al., 2021)	29	4.9	224	224	82.2
Hyb.	CvT-13 (Wu et al., 2021)	20	4.5	224	224	81.6
	CoAtNet-0 (Dai et al., 2021)	25	4.2	224	224	81.6
	LV-ViT-S (Jiang et al., 2021)	26	6.6	224	224	83.3
No-attn.	EAMLP-14 (Guo et al., 2021)	30	–	224	224	78.9
	ResMLP-S24 (Touvron et al., 2021a)	30	6.0	224	224	79.4
	gMLP-S (Liu et al., 2021a)	20	4.5	224	224	79.6
	GFNet-S (Rao et al., 2021)	25	4.5	224	224	80.0
	GFNet-H-S (Rao et al., 2021)	32	4.5	224	224	81.5
	AS-MLP-T (Lian et al., 2021)	28	4.4	224	224	81.3
	CycleMLP-B2 (Chen et al., 2021)	27	3.9	224	224	81.6
	ViP-Small/7 (Hou et al., 2022)	25	6.9	224	224	81.5
	S ² -MLPv2-Small/7 (Yu et al., 2021b)	25	6.9	224	224	82.0
	AST-Ti (Ours)	19	3.9	224	224	81.8
CNN	RegNetY-8G (Radosavovic et al., 2020)	39	8.0	224	224	81.7
	EfficientNet-B7 (Tan & Le, 2019)	66	39.2	600	600	84.3
	EfficientNetV2-M (Tan & Le, 2021)	54	25.0	480	480	85.1
Trans	PVT-B4 (Wang et al., 2021a)	62.6	10.1	224	224	83.6
	Swin-S (Liu et al., 2021b)	50	8.7	224	224	83.0
	Focal-S (Yang et al., 2021)	51	9.1	224	224	83.5
Hyb.	CvT-21 (Wu et al., 2021)	32	7.1	224	224	82.5
	CoAtNet-1 (Dai et al., 2021)	42	8.4	224	224	83.3
	LV-ViT-M (Jiang et al., 2021)	56	16.0	224	224	84.1
No. attn	MLP-mixer (Tolstikhin et al., 2021)	59	11.6	224	224	76.4
	EAMLP-19 (Guo et al., 2021)	55	–	224	224	79.4
	S ² -MLP-deep (Yu et al., 2022)	51	10.5	224	224	80.7
	CCS-MLP-36 (Yu et al., 2021a)	43	8.9	224	224	80.6
	GFNet-B (Rao et al., 2021)	43	7.9	224	224	80.7
	GFNet-H-B (Rao et al., 2021)	54	8.4	224	224	82.9
	AS-MLP-S (Lian et al., 2021)	50	8.5	224	224	83.1
	CycleMLP-B4 (Chen et al., 2021)	52	10.1	224	224	83.0
	ViP-Medium/7 (Hou et al., 2022)	50	16.3	224	224	82.7
	S ² -MLPv2-Medium/7 (Yu et al., 2021b)	55	16.3	224	224	83.6
	AST-S (Ours)	38	6.8	224	224	82.8
	AST-B (Ours)	53	10.2	224	224	83.2

Table 8: **Comparisons on ImageNet.** Our models are the most accurate within the “No. attn.” category. Hyb. = CNN+Transformer.

Method	Pre-train	Top-1 Acc. (%)	Top-5 Acc. (%)	Frames	Views	FLOPs $\times 10^9$
CNN models						
LGD-3D R101	IN-1k	81.5	95.6	–	–	–
SlowFast (Feichtenhofer et al., 2019)	-	80.4	94.8	8	10×3	3,180
SlowFast+NL (Feichtenhofer et al., 2019)	-	81.8	95.1	16	10×3	7,020
X3D-M (Feichtenhofer, 2020)	-	78.8	94.5	–	10×3	186
X3D-XL (Feichtenhofer, 2020)	-	81.9	95.5	–	10×3	1,452
Transformer and Hybrid models						
TimeSformer (Bertasius et al., 2021)	IN-1k	79.1	94.4	8	1×3	590
TimeSformer-HR (Bertasius et al., 2021)	IN-21k	81.8	95.8	8	1×3	590
TimeSformer-L (Bertasius et al., 2021)	IN-21k	82.2	95.6	96	1×3	7,140
ViViT-L/16x2 (Arnab et al., 2021)	IN-21k	82.9	94.6	32	4×3	17,352
Mformer (Patrick et al., 2021)	IN-21k	81.6	95.6	–	10×3	11,070
Mformer-HR (Patrick et al., 2021)	IN-21k	82.7	65.1	–	10×3	28,764
XViT-B (Bulat et al., 2021)	IN-21k	82.5	95.4	8	1×3	425
XViT-B (Bulat et al., 2021)	IN-21k	84.5	96.3	16	1×3	850
MViT-B (16×4) (Fan et al., 2021)	-	82.1	95.7	16	1×5	352
MViT-B (32×3) (Fan et al., 2021)	-	83.4	96.3	32	1×5	850
Swin-B (Liu et al., 2021c)	IN-21k	84.0	96.5	–	4×3	3,384
Swin-L (384) (Liu et al., 2021c)	IN-21k	86.1	97.3	–	10×5	105,350
MLP models (Attention-free transformers)						
VAST-Ti (Ours)	IN-1k	82.8	94.5	8	1×3	98
VAST-S (Ours)	IN-1k	84.0	95.5	8	1×3	169

Table 9: Comparison with CNN-based methods and state-of-the-art video transformers on Kinetics-600. Our tiny model VAST-Ti-8 outperforms the lightest version of MViT (+0.7%) while utilizing 4 \times fewer FLOPs, and even outperforms the most efficient version of XViT (+0.3%) while utilizing less than 4 \times fewer FLOPs.

Method	Pre-train	Top-1 Acc. (%)	Top-5 Acc. (%)	Frames	Views	FLOPs $\times 10^9$
CNN models						
bLVNet (Fan et al., 2019)	-	73.4	91.2	24×2	3×3	840
STM (Jiang et al., 2019)	IN-1k	73.7	91.6	16	-	-
TEA (Li et al., 2020)	IN-1k	76.1	92.5	16	10×3	2,100
TSM (R50) (Lin et al., 2019)	IN-1k	74.7	-	16	10×3	650
I3D NL	IN-1k	77.7	93.3	128	10×3	10,800
CorrNet-101	-	79.2	-	32	10×3	6,700
ip-CSN-152	-	79.2	93.3	8	10×3	3,270
LGD-3D R101	-	79.4	94.4	16	-	-
SlowFast (Feichtenhofer et al., 2019)	-	78.7	93.5	8	10×3	3,480
SlowFast (Feichtenhofer et al., 2019)	-	79.8	93.9	16	10×3	7,020
X3D-S (Feichtenhofer, 2020)	-	72.9	90.5	-	10×3	58
X3D-L (Feichtenhofer, 2020)	-	76.8	92.5	-	10×3	551
X3D-XXL (Feichtenhofer, 2020)	-	80.4	94.6	-	10×3	5,823
Transformer models						
TimeSformer (Bertasius et al., 2021)	IN-1k	75.8	-	8	1×3	590
TimeSformer (Bertasius et al., 2021)	IN-21k	78.0	93.7	8	1×3	590
TimeSformer-L (Bertasius et al., 2021)	IN-21k	80.7	94.7	96	1×3	7,140
ViViT-B/16x2 (Arnab et al., 2021)	IN-21k	78.8	-	32	4×3	3,408
ViViT-L/16x2 (Arnab et al., 2021)	IN-21k	80.6	94.7	32	4×3	17,352
Mformer Patrick et al. (2021)	IN-21k	79.7	94.2	-	10×3	11,070
Mformer-HR (Patrick et al., 2021)	IN-21k	81.1	95.2	-	10×3	28,764
XViT-B (Bulat et al., 2021)	IN-21k	78.4	93.7	8	1×3	425
XViT-B (Bulat et al., 2021)	IN-21k	80.2	94.7	16	1×3	850
MViT-S (Fan et al., 2021)	-	76.0	92.1	-	1×5	165
MViT-B (16×4) (Fan et al., 2021)	-	78.4	93.5	16	1×5	352
MViT-B (64×3) (Fan et al., 2021)	-	81.2	95.1	64	3×3	4,095
En-VidTr-S (Zhang et al., 2021)	IN-21k	79.4	94.0	8	10×3	3,900
En-VidTr-M (Zhang et al., 2021)	IN-21k	79.7	94.2	16	10×3	6,600
En-VidTr-L (Zhang et al., 2021)	IN-21k	80.5	94.6	32	10×3	11,760
Swin-T (Liu et al., 2021c)	IN-1k	78.8	93.6	-	4×3	1,056
Swin-S (Liu et al., 2021c)	IN-1k	80.6	94.5	-	4×3	1,992
Swin-B (Liu et al., 2021c)	IN-1k	80.6	94.6	-	4×3	3,384
Swin-L (384) (Liu et al., 2021c)	IN-21k	84.9	96.7	-	10×5	105,350
MLP models (Attention-free transformers)						
VAST-Ti (Ours)	IN-1k	78.0	93.2	8	1×3	98
VAST-Ti (Ours)	IN-1k	79.0	93.8	16	1×3	196
VAST-S (Ours)	IN-1k	78.9	93.8	8	1×3	169
VAST-S (Ours)	IN-1k	80.0	94.5	16	1×3	338

Table 10: Comparison with CNN-based methods and state-of-the-art video transformers on Kinetics-400. Our tiniest model VAST-Ti-8 largely outperforms the lightest MViT (+2%) while utilizing $2\times$ fewer FLOPs, and it is only 0.4% behind than the lightest XViT while utilizing less than $4\times$ fewer FLOPs. Our biggest model VAST-S-16 matches the best XViT model while utilizing less than $2\times$ fewer FLOPs.